

POLITECNICO DI TORINO

MASTER OF SCIENCE IN PHYSICS OF COMPLEX SYSTEMS

MASTER DEGREE THESIS

Zero-Risk Society



Politecnico
di Torino

ETH zürich



Université
de Paris

Supervisor:

Prof. Didier Sornette, ETH Zürich
PhD. Giuseppe Maria Ferro, ETH Zürich
Prof. Luca Dall'Asta, Politecnico di
Torino

Author:

Giuseppe Aventaggiato

ACADEMIC YEAR 2020-2021

Abstract

Modern society is going through a period of profound stagnation, obsessed with the necessity of controlling and removing any potential risk; we live in a “zero-risk society”. The present work aims to model and describe a phase transition at the social level from a risk-seeking environment to a risk-averse social mindset. Considering an investment scenario where financial capitals of agents evolve through an exponential Ornstein-Uhlenbeck stochastic process, we detailed the cyclic consequences of investment decisions in risk avoidance spreading and, vice versa, the opinions’ reverberation on investments. Monte Carlo evolution of an appropriate constrained time-dependent random field XY model illustrates the dynamics of individual risk propensities. The former is affected by the simultaneous influence of idiosyncratic risk inclinations, weighted social interactions at the local and global scale and mass media impact, based on opportunistic management by extremes. The introduction of suitable control parameters to trace the evolution of human society from early 1900 to present and future days revealed the model’s capability to predict the hypothesized social phase transition.

Acknowledgements

First of all, I wish to express my sincere gratitude to my supervisor, Professor Didier Sornette, for his valuable support and guidance in this exciting work. In addition to his brilliant professionalism and encyclopedic wisdom, he was a beacon of inspiration, leading me into the beauty of science and research. His help was a precious gem for my professional and personal growth.

I am extremely grateful to my supervisor, PhD. Giuseppe Maria Ferro, for his open-minded and highly skilled approach. He supported me in consciously exploring multiple theoretical solutions for the model's design, always present for discussing new viewpoints and resolving technical troubles.

Many thanks to my friend and colleague, Francesco Maria Russo, who worked with me on the project in Zurich. It was such an exciting experience to collaborate with him, walking through the numerous analytical difficulties, untying the computational knots and finally celebrating the working project and its results.

Special thanks to my wonderful family that always believed and encouraged me in my adventures, to whom I dedicate this thesis.

I could not have completed this project without my friends and their support in these very intense academic years. Beyond the physical distances, they constantly made me feel important and deeply motivated to pursue my objectives; always ready to help me overcome stressful periods, I spent my best lighthearted moments with them.

Contents

1	Introduction	8
1.1	Trapped in the zero-risk society	8
1.2	Model structure	9
2	Wealth evolution	11
2.1	Expected Utility theory (EUT)	11
2.2	Risk aversion	11
2.3	Individual portfolio optimization	13
2.4	Ergodicity problem in economics	14
2.5	Exponential Ornstein-Uhlenbeck process	15
3	Spreading of Opinions	18
3.1	Collective models for social dynamics	18
3.1.1	Random Field Ising Model	18
3.1.2	Majority vote model	19
3.2	Random field XY model	20
3.3	Wealth distribution	21
3.4	No access to opportunities	22
3.5	Idiosyncratic fields	23
3.6	Network	24
3.6.1	Introduction to graph theory	24
3.6.2	Scale free network	25
3.7	Social interactions	26
3.7.1	Interaction strength	26
3.7.2	Local network	27
3.7.3	Social network	27
3.7.4	Complete network	29
3.8	Media effect	29
3.9	Control parameters	31

4 Simulations	32
4.1 Model dynamics	32
4.2 Results	33
5 Covid model	36
6 Conclusion and perspectives	39
Bibliography	40

List of Figures

2.1	Example of utility functions U with respect to reward x for a risk-averse (green), a risk-neutral (blue) and a risk-seeking (red) agent. \bar{x} =expected reward, E=expected value, RP=risk premium, CE=certainty equivalent.	12
2.2	Time evolution of $Ln(W)$ under an Ornstein–Uhlenbeck process for $\theta = 0.1$, $\hat{\sigma} = 0.3$, initial condition $Ln(W)(t = 0) = -5$ and different values of $\hat{\mu} = \mu$	16
2.3	Log-normal distribution for wealth update with different values of the parameters μ and σ	17
3.1	Fisk Log-logistic distribution for $\alpha = 1$ and several values of β	22
3.2	Probability of having access to opportunities as function of the wealth. W.P.T. = 0.5, slope=0.1.	23
3.3	Local Network of 81 agents for Fisk wealth distribution with $\alpha = 1$, $\beta = 2.2$ and $q = 0.6$	28
3.4	Social Network of 81 agents for Fisk wealth distribution with $\alpha = 1$ and $\beta = 2.2$	28
3.5	Complete Network of 81 agents for Fisk wealth distribution with $\alpha = 1$, $\beta = 2.2$, $q = 0.6$ and $MC = 0.5$	29
4.1	Initial spin configuration for 100 agents. Magenta spins do not invest.	33
4.2	Average risk propensity vs <i>gamma media</i> , for different values of <i>media connectivity</i> and β in Fisk distribution. <i>Poverty threshold</i> = 0.05.	34
4.3	Average risk propensity vs <i>Poverty threshold</i> , for different values of <i>media connectivity</i> and <i>gamma media</i> . $\alpha = 1$ and $\beta = 2.2$ in the Fisk wealth distribution.	34
4.4	Average risk propensity in several historical periods.	35
5.1	SIRD model states and possible transitions.	37

List of Tables

3.1	Mapping between zero-risk society ingredients and XY model control parameters.	31
5.1	Parallelisms between Zero-risk society model and Covid model	38

Chapter 1

Introduction

1.1 Trapped in the zero-risk society

The modern world society is going through a period of demographic, economic, technological, institutional, cultural, and intellectual stagnation [1]. We live in a “zero-risk society”, a culture obsessed with the necessity of controlling and removing any risk. While the technological and sanitary improvements contribute to developing the wellness of our lives, bold risk-taking remains a fundamental constituent of a resilient civilisation. Indeed we are diving into a definitely out of equilibrium system where extreme events referred to as dragon kings [2] with exogenous nature like supervolcano eruptions, earthquakes or pandemics together with endogenous ones like market bubbles or terrorist uprisings constantly threaten the stillness of human existence. These know unknowns and many other unknown unknowns require a progressive, explorative avantgarde society to be faced. Dazzled by the apparent technological innovations of modern times, the nowadays citizens do not realise how they lack the massive and revolutionary impact of previous centuries discoveries. Moreover, the modern wealthy and aged civilisation reveals decadent lassitude regarding intellectual, cultural and social growth. There are five deep reasons to which the stagnation of human society has to be attributed:

1. Risk aversion as a consequence of increasing wealth and aging (welfare improvement).
2. Herding and imitation through social media.
3. Management shaped by extremes and overreaction.
4. Increasing inequality with a growing proportion of citizens that have no or less access to opportunity.
5. Technology creating an ‘illusion of control’.

The spread risk-averse mindset permeating the contemporary world necessitates a profound social and educational change in order to be uprooted from modern culture. Therefore, the crucial solution to transform the actual zero-risk society is to promote risk-taking experiences, new research activities, and long-term untargeted projects, even if they could seem meaningless. Society should facilitate access to opportunities for the entire population. By considering failure as an essential part of the learning process, strongly explorative and creative minds should become new influencers for the young generations. In this way, modern civilisation will face a period in which discoveries and inventions will support technological innovation, in a risk-taking scenario ready to deal with the new unpredictable challenges of the future.

1.2 Model structure

Inspired by the exciting phase transitions observed in several Ising-like models of statistical mechanics, the present Master Thesis aims to design a physical model capable of describing the transition of human society from a risk-taking world to a zero-risk social environment. In particular, we considered a population of N interacting agents that dynamically invest a fraction of their wealth in a risky explorative asset according to their risk propensities. To be precise, we should say that we considered “myopic agents”, i.e. agents neglect subsequent investment periods when investing at time t . After each investment, agents receive a gain or loss whose extent depends on the wealth allocated to the risky solution and, later on, update their opinions (in terms of risk propensity) by interacting with both their personal connections both the worldwide social networks. Mass Media would play a key role in shaping ideas spreading a distorted, fearful and unrealistic picture of the actual events with opportunistic purposes. Therefore the model represents a cyclic dynamical evolution in which investment decisions and the following realisations influence the ideas spreading mechanism that correctly determines an alteration of risk-aversion and, consequently, new investment decisions. Introducing suitable control parameters to scan human history, this two-layer structure characterised by the alternation of wealth evolution and opinions’ dynamics will reveal how the previously discussed factors [1-5] pushed the society toward a substantial reduction of the average risk propensity.

We start our analysis in chapter 2 with a brief introduction to state of the art in decision theory and portfolio optimisation, presenting the ergodicity problem in economics and discussing the choice of an appropriate stochastic process to represent wealth evolution in a dynamical investment environment. Chapter 3 is devoted to the core component of the present Master Thesis, the design of a constrained random field time-dependent XY model that mimics opinions’ spreading in an interacting social system with massive media influence. After analysing how wealth distribu-

tion and inequality changed in human history during the last decades, we propose an insightful description of social media interactions and media management by extremes. Successively in Chapter 4, we combine the wealth evolution mechanism with the XY Montecarlo dynamics for the diffusion of ideas and report the coherent results of intensive numerical simulations. Chapter 5 presents an inspiring application of the model to the Covid19 pandemic, highlighting why the social response has been significantly different from other similar epidemics in the past. Chapter 6 is devoted to the conclusion and perspectives. The current research project has been entirely developed at ETH Zurich in collaboration with my friend and colleague Francesco Maria Russo who dedicated his Master Thesis to detail the theoretical conjectures and experimental results of the Covid version of the model.

Chapter 2

Wealth evolution

2.1 Expected Utility theory (EUT)

In economics, the utility function is a mathematical function that ranks consumption goods by assigning a number to each where larger numbers indicate preferred goods. Utility represents the satisfaction or pleasure that customers receive for consuming a good or service. As discussed in [3] the expected utility theory represents the famous first attempt to describe how individual decision making violates the expected value criterion according to which the investment decision should be based on the average value of the asset's return. On the contrary, Expected Utility Theory (EUT) states that the decision-maker chooses between risky or uncertain prospects by comparing their expected utility values.

2.2 Risk aversion

In the framework of individual decision-making, risk aversion refers to the psychological tendency to prefer a situation with a highly predictable payoff rather than a more unpredictable option, even with a possibly greater profit. Considering that an agent has to choose between a guaranteed return and a risk reward with the same average values, risk aversion is quantified by the difference in the average utility of the two alternatives. In this frame, the certainty equivalent represents the minor payoff that an individual would be indifferent to spending on a gamble or guarantee, while the risk premium is the difference between the expected value of the reward and the certainty equivalent. As a trivial consequence of Jensen's inequality, the former description can be embedded in the concavity of the utility function. Therefore, while the utility functions of a risk-seeking agent and a neutral one are convex and linear, respectively, a risk-averse individual has a concave utility function as displaced in figure 2.1. Therefore, an opportunely weighted (to overcome invariance

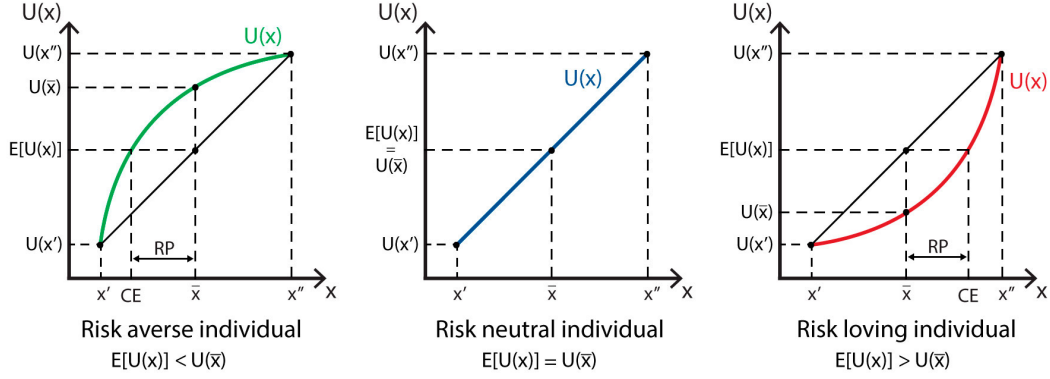


Figure 2.1: Example of utility functions U with respect to reward x for a risk-averse (green), a risk-neutral (blue) and a risk-seeking (red) agent. \bar{x} =expected reward, E =expected value, RP =risk premium, CE =certainty equivalent.

under affine transformations of the utility function) version of the utility curvature can be adopted to describe different types of risk avoidance. Kenneth Arrow (1971) [4] and John Pratt (1965) defined the following two measures of risk aversion:

- Absolute risk aversion:

$$R_A(W) = -\frac{U''(W)}{U'(W)} \quad (2.1)$$

with W representing the wealth level and $U'(W), U''(W)$ the first and second derivatives of the utility function respectively. In case $R_A(W)$ is an increasing function of the wealth the agent has an increasing absolute risk aversion (IARA), namely she decides to allocate a fewer absolute amount of wealth to the risky asset as her wealth increases. Instead, an agent with decreasing absolute risk aversion (DARA) will invest more money in the risky asset as her wealth increases. The amount devoted to the uncertain investment will be invariant by wealth changes for a constant absolute risk averse (CARA) individual.

- Relative risk aversion:

$$R_R(W) = -W \frac{U''(W)}{U'(W)} \quad (2.2)$$

This measure describes how the relative amount of wealth invested in a risky asset changes with respect to a change in the total wealth, for example an increasing relative risk-averse (IRRA) agent will allocate a smaller fraction of her money in the risky asset while her wealth increases.

2.3 Individual portfolio optimization

Consider an agent with wealth W who can invest in two assets, a risk free asset with return $r_0 = 0$, and a risky asset with random return $r \in [-1, \infty[$:

$$r = \begin{cases} +g, & \text{with probability } p \\ -l, & \text{with probability } 1 - p \end{cases} \quad (2.3)$$

With $g \geq 0, 0 \leq l \leq 1$ and such that $E[r] = pg + (1 - p)(-l) > r_0$. The latter condition ensures that the investor should purchase some risky asset (no matter how risk averse she might be). If the agent invests the (absolute) amount k in the uncertain solution, she gets in period 1 :

$$(W - k)(1 + r_0) + k(1 + r) = W + kr = W \left(1 + \frac{k}{W}r \right) = W(1 + ar)$$

Where $a = \frac{k}{W}$ is the fraction of wealth devoted to the risky option. According to the EUT she will decide the amount of wealth to allocate to the risky investment considering the following optimization problem:

$$\begin{aligned} a^* &= \max_a V(a) = \max_a E[U(W(1 + ar))] \\ 0 &\leq a \leq 1 \text{ (no short-selling and no borrowing)} \end{aligned} \quad (2.4)$$

Therefore the individual portfolio optimization results to be intensely dependent on the functional shape of the utility function. In the framework of our model, we describe individual portfolio optimization mechanism through a ‘‘power risk aversion’’ utility function [5] of the form:

$$U(W) = \frac{1}{\gamma} \left[1 - \exp \left(-\gamma \left(\frac{W^{1-\sigma} - 1}{1 - \sigma} \right) \right) \right], \sigma \geq 0, \gamma \geq 0 \quad (2.5)$$

The set of parameters reproducing commonly observed investment choices in the present society is $\gamma > 0$ and $0 < \sigma < 1$ for which the agent, as wealth increases, will increase her risky investment in absolute terms (DARA) while reducing it in relative ones (IRRA) [4]. Consequently, the optimal (absolute) allocation of wealth k^* to the uncertain option that derives from Eq. 2.4, assuming utility function in Eq. 2.5 and return distribution of Eq. 2.3 satisfies the following relation:

$$\left(\frac{pg}{(1-p)l} \right)^{\frac{1}{\sigma}} \left(\frac{W - k^*l}{W + k^*g} \right) = \exp \left\{ -\frac{\gamma}{\sigma(1-\sigma)} [(W - k^*l)^{1-\sigma} - (W + k^*g)^{1-\sigma}] \right\} \quad (2.6)$$

Taking profit of several numerical simulations with different risky asset’s specifics and numerous utility parameters, we inferred the general evolution of the absolute amount devoted to the risky asset to be of the form:

$$k^*(W) \approx const * W^\sigma \quad (2.7)$$

2.4 Ergodicity problem in economics

The ergodic hypothesis is a key analytical device of equilibrium statistical mechanics [6]. It is based on the assumption that the time average and the expectation value of an observable coincide. When valid, this assumption allows to replace dynamical descriptions with much simpler probabilistic ones, but the conditions for validity are restrictive, even more so for non-equilibrium systems. Often in economics, the analysis of wealth evolution through multiple investments has been conducted by assuming ergodicity, thus replacing wealth with its expected value before computing the dynamic time growth. This completely incorrect hypothesis will naturally lead to experimental results enormously different from theoretical predictions unveiling the exponential nature of wealth evolution [7]. For example, let us consider an agent with initial wealth W_0 that invests in a lottery with return X_1 :

$$X_1 = \begin{cases} 2 & \text{w. p. } 1/2 \\ q & \text{w. p. } 1/2 \end{cases} \quad 0 < q < 1/2 \quad (2.8)$$

The expectation value of her capital W_n after n bets in the same game with repeated allocation of the whole accumulated wealth at each time will be:

$$E[W_n] = (1 + q/2)^n W_0 \quad (2.9)$$

that seems to grow exponentially over time. However using the strong law of large numbers (SLLN) [8] it's possible to show that the capital typically vanish exponentially. Indeed:

$$\frac{1}{n} \log(W_n/W_0) = \frac{1}{n} \sum_{i=1}^n \log X_i \rightarrow E[\log X_i] = \frac{1}{2} \log(2q) \quad (2.10)$$

This means that almost surely

$$W_n \simeq W_0 e^{-cn}, \quad c = \frac{1}{2} |\log(2q)| > 0 \quad (2.11)$$

For all $a > 0$:

$$P\{W_n > a\} \rightarrow 0 \text{ as } n \rightarrow \infty \quad (2.12)$$

Therefore, in the investment scenario illustrated in section 2.3, in which the agent faces a choice between a riskless and a risky asset, the non-ergodicity problem plays a significant role. Actually, for any fraction of wealth repeatedly allocated to the risky option, an exponential wealth evolution leads the individual capital to either an unbounded growth or a collapse to zero depending on the assets' features.

2.5 Exponential Ornstein-Uhlenbeck process

As discussed in the introductory section, the present model’s primary purpose is to analyse how individual risk propensity changes in an investing society characterised by an intensive network of interactions in which media affect decision-making through a distortion of real news (management by extremes). In this framework, the dynamical evolution of wealth resulting from the probabilistic returns of financial assets should not undergo an uncontrolled exponential drift. On the contrary, the introduction of the investment panorama serves merely as a proxy for evaluating how risk aversion influence human choices and, conversely, how random realisations of external events can affect the individual propensity to take a risk. Therefore, a more realistic description of the wealth distribution among the whole population should be based on stationarity. The latter ensures a dynamic progression of the individual capitals such that at each step of investment, the asset’s return can produce a gain or a loss for any agent, but the final wealth distribution remains quite similar to the initial one. Keeping in mind the association between risk propensity and actual wealth fraction invested in a risky option, both represented by the parameter a in our model, we will practically let the individual wealth evolve with a stochastic process, guaranteeing the achievement of a stationary distribution (for further analysis, the consequences of short time scales preventing equilibration could be examined). Indeed, the use of a stochastic process is a coarse-grained description of a sequential optimization problem performed by myopic agents in a time period “short enough” such that the assumption of stationary average wealth is reasonable. Although the volatility of financial assets prices could be evaluated through an appropriate Ornstein-Uhlenbeck process [9], in the present Thesis, we decided to adopt the more involved treatment introduced by Eduardo Schwartz to calibrate the evolution of commodity prices [10]: the exponential Ornstein–Uhlenbeck process, that ensures the wealth acquires only non-negative values. During this stochastic dynamics of the capital $W(t)$ under the white noise $X(t)$ described by the equation:

$$dW(t) = \theta\{\hat{\mu} - \text{Ln}[W(t)]\}W(t)dt + \hat{\sigma}W(t)dX(t) \quad (2.13)$$

the logarithm of the individual wealth evolves through a standard Ornstein–Uhlenbeck process as reported in figure 2.2 for $\theta = 0.1$, $\hat{\sigma} = 0.3$, initial condition $\text{Ln}(W)(t = 0) = -5$ and several values of $\hat{\mu} = \mu$. Note that, to be able to define its logarithm, wealth will be adimensionalized and expressed in units of a characteristic wealth level ($W = 1$) corresponding to the most probable value of the Fisk distribution from which the capitals of the population will be sampled, as discussed in the following sections. Since in stationary conditions, the logarithm of the wealth amount will be distributed according to a Gaussian probability function with average μ and standard deviation σ , the wealth stationary distribution will be log-normal of the

form:

$$P(W) = \frac{1}{W\sigma\sqrt{2\pi}} \exp\left(-\frac{(\ln W - \mu)^2}{2\sigma^2}\right) \quad (2.14)$$

as displaced in picture 2.3. Indeed, for any agent, after the allocation of the wealth fraction a to the risky asset, we will evaluate the new wealth sampling from the log-normal distribution in which μ and σ parameters have been tuned such that:

$$E[W] = \exp\left(\mu + \frac{\sigma^2}{2}\right) = W_0 \quad (2.15)$$

$$STD[W] = \sqrt{[\exp(\sigma^2) - 1] \exp(2\mu + \sigma^2)} = aW_0 \quad (2.16)$$

The new wealth will be sampled from a distribution with an average value equal to the initial wealth (Eq. 2.15) and standard deviation represented by the absolute amount of wealth devoted to the risky asset (Eq. 2.16), expressed in terms of initial wealth capital. Hence a risk-seeking individual (large a) will invest many resources in the risky option and have a significant standard deviation in the future wealth distribution; namely, she could receive a notable gain or face a terrible loss. Instead, a conservative risk-averse agent (small a) will exhibit a new wealth that slightly oscillates around its original value.

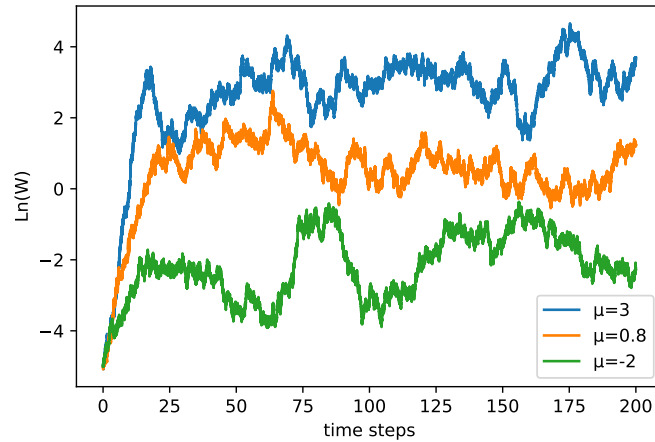


Figure 2.2: Time evolution of $\ln(W)$ under an Ornstein–Uhlenbeck process for $\theta = 0.1$, $\hat{\sigma} = 0.3$, initial condition $\ln(W)(t = 0) = -5$ and different values of $\hat{\mu} = \mu$.

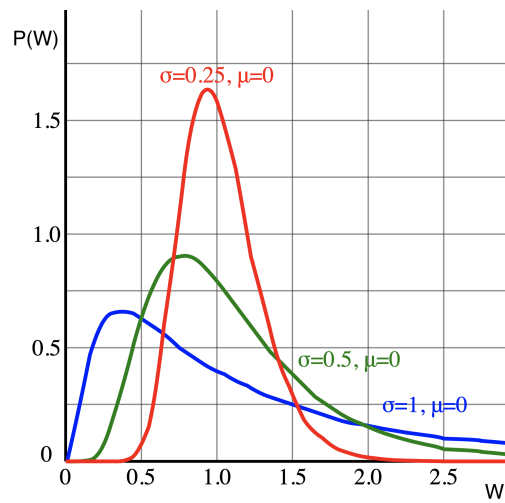


Figure 2.3: Log-normal distribution for wealth update with different values of the parameters μ and σ .

Chapter 3

Spreading of Opinions

3.1 Collective models for social dynamics

Traditional macroeconomics often assume that the collective behaviour of interconnected decision-makers can be expressed in terms of a representative agent embodying and simplifying the group's heterogeneity. In 1992, Kirman [11] strongly criticised this position, considering it misleading and inadequate to capture collective trends with massive macro-scale consequences. In this context, the Random Field Ising Model (RFIM) and the Majority vote model appeared as insightful solutions to capture the complexity of opinions dynamics in an interacting network where, albeit the simple behaviour of the single agent, powerful critical social choices can arise [12].

3.1.1 Random Field Ising Model

The Random Field Ising model (RFIM) represents an insightful description of the natural stochasticity permeating solid-state physics. Indeed, quenched randomness characterises all solid materials, either in terms of impurities and defects or as fundamental structural properties like those exhibited by alloys and glasses [13]. Therefore, a complete understanding of the functional behaviour of solids must include a random contribution; this is well exemplified by RFIM, where long-range interactions compete with random ordering fields. The one dimensional Hamiltonian of the model is:

$$H = - \sum_{\langle i,j \rangle} J_{ij} s_i s_j - \sum_i h_i s_i \quad (3.1)$$

where the spin variable $s_i \in \{-1, 1\}$, J_{ij} represents attractive or repulsive interaction between spins i and j while the fields h_i are independent random variables with symmetric distribution, usually gaussian or bimodal. The first and second summations run over all the couples of interacting spins and over all the spin variables,

respectively. The RFIM revealed interesting nonequilibrium and dynamic phase-transition properties under the influence of periodically oscillating random fields, as analysed by Yüksel et al. [14] in a simple cubic lattice with effective field theory and by Acharyya [15] through a Monte Carlo simulation on a two-dimensional grid. In 2005 Michard and Bouchaud [16] showed the possibility to adopt RFIM to reveal the implications of social pressure and imitation together with public information in interesting collective effects like birth rates, decay of applause or sales of mobile phones. In the following, we will investigate the dynamical evolution (through free energy minimisation) of the XY model, a generalisation of RFIM where continuous unary vectors substitute spin variables [17]. In this framework, each variable embodies agent decision; field terms stand for individual opinions or media influences while the couplings J_{ij} account for social herding.

3.1.2 Majority vote model

An alternative description for opinion dynamics in a population is the Majority vote model, where individual preferences are encoded in the spin variables $\sigma = \pm 1$, placed on the sites of a regular lattice [18]. At each time step, a spin is randomly picked, and it adopts the majority sign of the neighbouring spins with probability p and the minority with probability $q = 1 - p$. Formally the i -th spin flip probability can be expressed by

$$w_i(\sigma) = \frac{1}{2} \left[1 - (1 - 2q)\sigma_i S \left(\sum_{\delta} \sigma_{i+\delta} \right) \right] \quad (3.2)$$

where the summation runs over all the neighbouring variables of spin i , S is defined as $S(x) = \text{sign}(x)$ if $x \neq 0$ and $S(0) = 0$. Intensive Monte Carlo simulations and finite sizes analyses [18] revealed that the majority vote model exhibits a second-order phase transition at the critical noise value $q_c = 0.075$ with the equivalent critical exponents of the square Ising model with periodic boundary conditions. Therefore the isotropic majority vote model has the same universal critical behaviour as the equilibrium Ising model. The corresponding result has been observed in the simulation of a square lattice majority vote model with strong opinions individuals that influence the neighbouring sites more than normal agents [19]. Thus, although the universality class features of the Ising model are preserved, an increasing concentration of individuals with stronger opinions weakens the consensus of the network, reducing the critical noise value for the transition from ordered to disordered state. Furthermore, a generalization of the spin variables to two-dimensional normalized rotators on a square lattice [20] revealed the presence of low-noise Kosterlitz-Thouless like phase [21] where the measured correlation function exponent depends on the noise and the system is critical in the sense that the correlation length is infinity.

The Majority vote model provided robust results in the description of group dynamics and correctly reported collective social phenomena like the consequences of global and local mass media influence [22].

3.2 Random field XY model

In order to describe the transition of human societies to a zero-risk scenario portrayed by a diffused risk avoidance, we designed an XY model constrained in the first quarter (with all spins having an angle between 0 and $\pi/2$) with time-dependent random fields [17]. This model represents the fundamental structure on which diffused social interactions and media hype and exaggeration, together with a consistent fraction of humans with no access to opportunities, can alter the individual risk propensity freezing the entire society in a stagnation condition. Let us consider a system where N interacting agents with the same utility function but different wealth perform a portfolio optimization choice among a risky and riskless asset. In this framework, the agent's decision can be encoded in the 2-dimensional spin variable:

$$\vec{s}_i = (\sqrt{a_i}, \sqrt{1 - a_i}), \quad \|\vec{s}_i\| = 1 \quad (3.3)$$

where a_i is the fraction of wealth invested in the risky asset by agent i . Therefore, the first (respectively second) component of the spin encodes the relative amount of the wealth allocated to the risky (respectively riskless) option. At each time step t the Hamiltonian of the system will be of the form :

$$H(t) = - \sum_i \vec{h}_i(t) \cdot \vec{s}_i - \sum_{\langle ij \rangle} J_{ij} \vec{s}_i \cdot \vec{s}_j - \sum_i \vec{h}_{\text{media},i}(t) \cdot \vec{s}_i \quad (3.4)$$

where the summations on the index i run over all the agents in the system while the sum on $\langle ij \rangle$ takes into account all the possible spin couples of the network. The idiosyncratic field $\vec{h}_i(t)$ represents the individual preference over the two assets of agent i if considered in isolation at time t . Furthermore, the couplings J_{ij} display the social interactions through imitation and herding while the term $\vec{h}_{\text{media},i}(t)$ encodes the media influence that modify individual mindset of agent i at time t , especially pushing toward fearful risk-averse thinking (as will be discussed in the following sections). The time dependence of field terms in the Hamiltonian derives from the dynamical progression of wealth through the exponential Ornstein-Uhlenbeck process (for the moment kept at stationarity) modelling the probabilistic outcomes of the risky asset. During the numerical simulations, after each investment realisation, we will let opinions evolve through a Montecarlo dynamics based on the presented Hamiltonian, with temperature initially equal to zero, for the sake of simplicity. In this context temperature can be regarded as choice stochasticity, even in absence of

interactions. As a proxy for the population propensity to take risks, we consider the average fraction of wealth invested in the risky asset as the model order parameter:

$$\bar{a} = \frac{1}{N} \sum_{i=1}^N a_i \in [0, 1] \quad (3.5)$$

Therefore we analysed how the \bar{a} values change by varying opportune control parameters. In the following sections, the different ingredients of the Hamiltonian and their dependence on capitals' evolution will be detailed. Moreover, a profound note will be placed on the development of wealth distribution and inequality crosswise human history.

3.3 Wealth distribution

A fundamental ingredient specifying the evolution of human societies across different historical periods is the distribution of wealth among the population. If we refer to the US case study [23], albeit the functional form of the wealth histogram seems to be left unaltered over the last decades, two relevant phenomena have been observed [24]:

- a global shift of the average wealth illustrating how a diffused welfare truly characterizes the recent historical period that is a profound reason underlying the development and spreading of a risk-averse mindset;
- a growing wealth inequality represented by an increment in the tail of wealth distribution such that the share of the global wealth owned by the top 1% of the population increased from 25% in 1980 to 40% in 2016 [25].

A realistic function capable of capturing the main features of wealth distribution from national to global scale is the log-logistic distribution, in economics typically referred to as Fisk distribution [26]. It embodies the power-law behaviour of Pareto probability density function for large wealth values (necessary to encompass wealthy outliers) while preserving a good fitting for small wealth amounts like the log-normal distribution. The mathematical expression of the Fisk probability density function is:

$$P(W) = \frac{(\beta/\alpha)(W/\alpha)^{\beta-1}}{(1 + (W/\alpha)^\beta)^2} \quad (3.6)$$

with α being the scale parameter while β being the shape one. The functional shape of the distribution is displaced in figure 3.1. In the following analysis, we will tune both parameters to observe the consequences of wealth evolution in terms of diffusion of a zero-risk culture. Mainly we will explore the role of the parameter β , whose reciprocal form represents the Gini coefficient [27], a statistical measure of dispersion meant to describe wealth inequality.

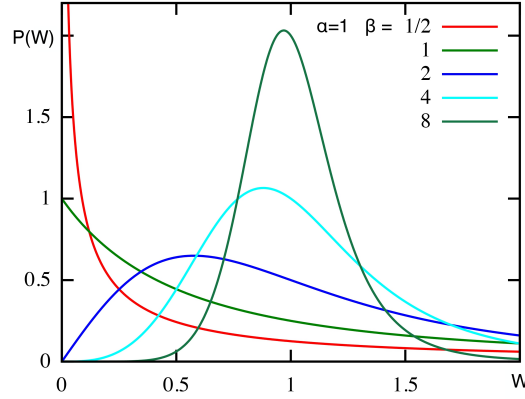


Figure 3.1: Fisk Log-logistic distribution for $\alpha = 1$ and several values of β .

3.4 No access to opportunities

As a consequence of the increasing wealth inequality among the population, a growing portion of citizens in western countries has no or limited access to investment and innovation opportunities. Sure enough, they face a harsh socio-economical condition, daily struggling for their own lives, suffering poverty and health problems, with no access to high-quality education. Deprived of an adequate intellectual background and, more relevant, constantly engaged in the risky challenges of their daily life experiences, these individuals can not explore investments to improve the proper social condition. Their attitudes and difficulties reflect in the XY model for opinions' spreading. Indeed, a set of spins representing the risk propensities of the poorest people with no access to opportunities point toward the vertical direction exhibiting a null fraction of wealth invested in the risky asset $a = 0$. This phenomenon strongly impacts the collective behaviour of the interacting network our society is involved in. Even if their influence is weak (as discussed in section 3.7.1) the citizens mentioned above contribute to changing the risk propensity of people they interact with, pushing their spins along the vertical direction (coupling terms in the Hamiltonian). We controlled the portion of people with no access to opportunities from the technical viewpoint by introducing the control parameter *Poverty Threshold* defined as the quantile of agents whose wealth lies below a “wealth poverty threshold” (W.P.T). The latter has been derived a posteriori by integration of the Fisk wealth distribution $P(W)$ in the form :

$$\int_0^{\text{W.P.T}} P(W)dW = \text{Poverty Threshold} \quad (3.7)$$

The transition in wealth from free access to risky opportunities to socio-economic exclusion from explorative investments should reveal a smooth shape. Therefore we exploited a sigmoid function centred in the wealth poverty threshold and with a sufficiently steep curvature to model the probability of accessing opportunities as a function of wealth. If we consider an agent i with wealth $W_i(t)$ at time t , her probability of having access to opportunities is:

$$P_i(\text{access to opportunities})(t) = \frac{1}{1 + \exp \frac{W.P.T - W_i(t)}{\text{slope}}} \quad (3.8)$$

In which W.P.T is the wealth poverty threshold while the slope parameter has been fixed to the default value 0.1. The latter functional formulation results in the behaviour shown in figure 3.2.

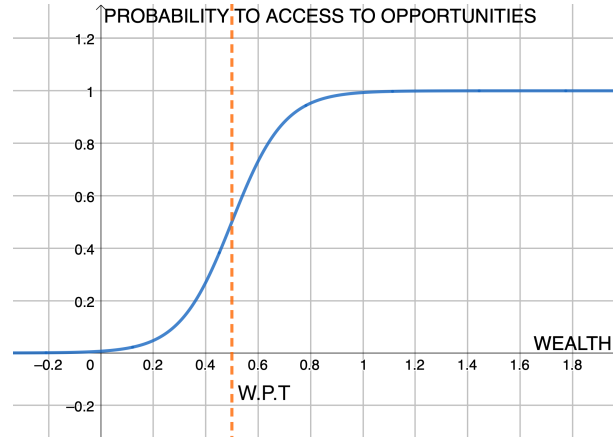


Figure 3.2: Probability of having access to opportunities as function of the wealth. W.P.T. = 0.5, slope=0.1.

3.5 Idiosyncratic fields

The first essential element characterizing the Hamiltonian of the random field XY model for opinions' spreading is the set of idiosyncratic fields encoding the individual risk propensity for any agent. If we consider the agent i with wealth $W_i(t)$ at time t her field $\vec{h}_i(t)$ will be given by:

$$\vec{h}_i(t) = \left(\sqrt{a_i^*(t)}, \sqrt{1 - a_i^*(t)} \right) W_i(t) \quad (3.9)$$

where $a_i^*(t)$ represents the fraction of wealth $W_i(t)$ invested by agent i in the risky asset at time t according to her portfolio optimization. Supposing an investment

scenario in which an agent with a DARA and IRRA utility function (as that of equation 2.5 for an appropriate choice of the parameters) has to optimally allocate her initial resources in a risky and a riskless assets, the portfolio optimization through EUT will lead to the result of equation 2.7. Therefore we can estimate the quantity $a_i^*(t)$ as:

$$a_i^*(t) = W_i(t)^{\sigma-1} \quad 0 < \sigma < 1 \quad (3.10)$$

where σ embodies and quantifies the IRRA character of the utility function. In our numerical simulations, we let $\sigma = 0.5$ since it does not represent a relevant control parameter for our discussion. Note that the field modulus is equal to the individual wealth $\|h_i\| = W_i$ accounting for the fact that richer people are less likely to be influenced and will stick to their personal preferences.

3.6 Network

A coherent model that vividly explains the opinions' dynamics in a population finds its fundamental roots in the network topology and couplings strengths. Therefore, before detailing the simulated social interacting system, we will devote the present section to introduce the principles underlying graph theory and scale-free network structures.

3.6.1 Introduction to graph theory

A directed graph (digraph) G is an ordered pair $G = (V, E)$ where V is called the set of vertices and $E \subseteq V \times V$ is called the set of edges. Self-edges (i, i) will not be allowed; that is $(i, i) \notin E$, ever. An undirected graph, sometimes called simply a graph, is $G = (V, E)$ where $E \subset V \times V$ is a subset of pairs of vertices in which opposite pairs $[(v, w)] = [(w, v)]$ are identified in a single equivalence class.

Although the wide variety of graph structures account for the description of several interacting systems, many physical models require a stochastic formalization of the network, namely a random graph. A random graph ensemble is a probability distribution over graphs [28], that is $P : G \mapsto P(G) \geq 0$ such that $\sum_G P(G) = 1$. If we consider distributions of graphs with fixed vertex set $V = \{1, \dots, n\}$, there are $m = n(n-1)/2$ potential edges on such vertex set, therefore the probability space is defined on a set of $2^{\frac{n(n-1)}{2}}$ possible structures.

Among the numerous families of random graphs common examples are the Erdős-Rényi $G(n, p)$ random graph with probability measure:

$$P(G) = p^{|E|} (1-p)^{\frac{1}{2}n(n-1)-|E|} \quad (3.11)$$

where each edge is inserted in the network with probability p and the Erdős-Rényi $G(n, m)$ random graph that is defined as the uniform probability space of graphs

with n vertices and m edges. For large n , $G(n, p = c/n)$ and $G(n, m = cn/2)$ behave very similarly, because the binomial distribution of the number of edges $P(|E| = m)$ characterising $G(n, p)$ concentrates sharply around its mean value.

3.6.2 Scale free network

A scale-free network [29] is identified by a power-law distribution of the degrees of nodes resulting in an organization where some individuals, the hubs, carry a massive number of links, effectively overcoming the others. In details, the fraction of network nodes with k neighbouring sites is expressed by:

$$P(k) \sim k^{-\gamma} \quad (3.12)$$

where the γ typically belongs to the range $2 < \gamma < 3$. These engaging networks with size-independent topological properties have been frequently adopted in biological models for protein-protein interaction, semantic networks [30], airline interactions and appeared appropriate to describe the internet and web graph of the World Wide Web. In order to build such an interesting topological structure, new nodes are iteratively added to the network with preferential attachment Π , namely a certain probability of a new node to be connected with sites already existing in the system. In this framework, an insightful example of a generative algorithm for a scale-free network is the Albert Barabási model [31], which begins with an initial connected set of m_0 nodes; progressively, a new node is added to the system and forms $m < m_0$ edges with the older variables. The preferential attachment probability Π_i to be connected with the pre-existing node i is:

$$\Pi_i = \frac{k_i}{\sum_j k_j} \quad (3.13)$$

where k_i represents the degree of node i and the sum runs over all the nodes already placed in the network. Therefore, heavily linked nodes tend to quickly accumulate a larger number of connected sites and eventually become the network hubs. In many physical circumstances, the introduction of individual properties of the single nodes provides a more realistic picture of the system beyond the approximation of identical agents. Bianconi-Barabási model [32] [33] attributes to each node an intrinsic and innate property called fitness which results in the individual capability of attracting links in the network (fitter nodes attract more edges than less fit ones). After designing an initially small and connected network, a new node carrying m links will be connected to the already existing site i with probability:

$$\Pi_i = \frac{\eta_i k_i}{\sum_\ell \eta_\ell k_\ell} \quad (3.14)$$

where η_i is the fitness of node i while k_i represents its degree and the sum runs over all the nodes already placed in the network. Fitness and degree jointly determine the attractiveness and evolution of a node. Hence, node i will increase its connectivity k_i at a rate that is proportional to the probability that a new link will attach to it, giving:

$$\frac{\partial k_i}{\partial t} = m \frac{\eta_i k_i}{\sum_j k_j \eta_j} \quad (3.15)$$

The time evolution of i -th node degree follows a power law growth:

$$k_{\eta_i}(t, t_0) = m \left(\frac{t}{t_0} \right)^{\beta(\eta_i)} \quad (3.16)$$

where the dynamic exponent β depends on the fitness parameter, and t and t_0 represent the actual and initial time step respectively.

3.7 Social interactions

3.7.1 Interaction strength

In modern world society, each agent steadily feels the pressure of the surrounding social environment that unavoidably modifies individual opinion and alters the consequent decision-making. In the present model, the social interaction between individual i with wealth W_i and agent j with wealth W_j is weighted by $1/2$ of the harmonic mean between the two wealth amounts:

$$J_{ij} = W_i // W_j = \frac{W_i W_j}{W_i + W_j} \quad (3.17)$$

This simple mathematical operation that mimics the parallel of resistors in electronics acquires a powerful meaning in an XY model where the intensity of personal opinion, namely the modulus of the idiosyncratic field, coincides with the individual wealth. The main properties of the chosen couplings can be valued in the following situations:

- $W_i \gg W_j \implies J_{ij} \approx W_j$

If a rich agent interacts with a poor one, their reciprocal influence is expressed as the wealth of the poorest. Therefore while poor people feel an influence from rich ones comparable with their own opinion, wealthy people feel a slight impact from poor compared with their individual belief. Consequently, a rich agent needs a remarkable number of links with poor people to change her mind.

- $W_i \approx W_j \implies J_{ij} \approx W_i/2$

If two individuals with similar wealth condition communicate, they feel a reciprocal influence quantifiable as half of their own ideas.

The chosen harmonic procedure to estimate social interactions deeply simplifies the network analysis since it both avoids introducing a directed graph (digraph) both prevents from the setting of an absolute and arbitrary reference to quantify the intensity of the links. While the strength of interpersonal interactions can be considered a constant quantity independent of the evolution of societies, a profound constituent describing the progress of human history is the diffusion of social media that removed geographical boundaries and budgetary classism from the opinions' spreading mechanism. We captured the expansion in connectivity of the modern world through the probabilistic superposition of a local and a social network.

3.7.2 Local network

Before the advent of Facebook, Instagram, Twitter, and many other social media channels, interpersonal communication at the half of the past century was dominated by a more restrictive network of private interactions mainly organized around the principle of homophily as illustrated by McPherson et al. [34]. This preferential connection principle relies on the idea that the social organization of a human community tends to promote aggregation of individuals sharing similar features like age, religion, gender, education and social classes. In particular educational, occupational and class homophily not only affect strong ties like marriage and friendship but have even a more profound impact on the less intimate social links, as pointed out by Verbrugge [35]. Based on the previous discussion, we firstly allocated wealth resources to the simulated population by sampling from the Fisk distribution and then designed a “local network” modelling the interactions in the pre-social media world according to wealth homophily. After sorting the agents by their prosperity levels such that $W_1 > W_2 > \dots > W_N$, we accept a link between agent i with wealth W_i and agent $i + k$ with lower wealth W_{i+k} with probability q^k . By setting $q = 0.6$ for a population of 81 interacting agents with Fisk wealth distribution ($\alpha = 1$ and $\beta = 2.2$), the local network has the structure displaced in figure 3.3. Note that the colours of the nodes are ranked according to personal wealth, such that dark blue agents are poor, light blue represent middle classes, while green, red and crimson are the more affluent individuals.

3.7.3 Social network

From the interconnectivity perspective, the dynamical evolution of human history can be interpreted as the superposition to the homophily based (wealth homophily) local network of a worldwide social network where news openly circulate, typically

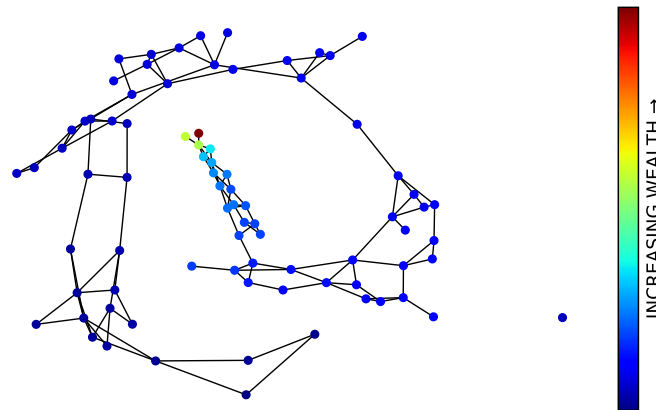


Figure 3.3: Local Network of 81 agents for Fisk wealth distribution with $\alpha = 1$, $\beta = 2.2$ and $q = 0.6$.

undergoing self-reinforcing mechanisms referred to as social media hypes [36]. We decided to model the social media global network with a scale free graph employing the generative Bianconi-Barabási model. In the present framework, we associate to the fitness parameter the amount of wealth each agent owns, mimicking the fact that richer individuals are typically highly connected and can shape opinions of the poorer social classes. As described by the fitness model's procedure, we started the network with a small cluster of interconnected wealthy people and then iteratively added a node with m (default $m=2$) links. The social network processed with the former procedure is shown in figure 3.4 for a population with 81 individuals with the same wealth distribution and colours' legend of the previous section 3.7.2. As expected, richest people (red and green dots) possess the largest number of interactions.

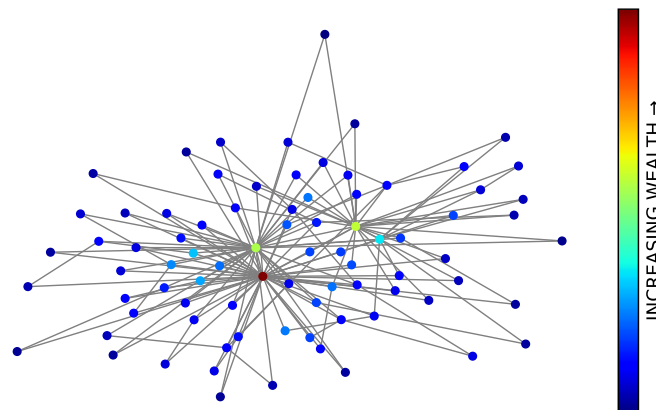


Figure 3.4: Social Network of 81 agents for Fisk wealth distribution with $\alpha = 1$ and $\beta = 2.2$.

3.7.4 Complete network

We described the complete interactions of a realistic community as the superposition of interpersonal communications based on wealth homophily and social media connections. Starting from a local network we scanned all the edges of the social media adjacency matrix and, if not already present in the local network, we included them with probability equal to the control parameter *media connectivity*(MC). The latter symbolises a simple and efficient way to scan human history analysing the role of connectivity in information dynamics and risk avoidance spreading. In particular, in the past, only the local network was available ($MC = 0$) and over time the *media connectivity* has increased. The resulting network for 81 agents with $MC = 0.5$ and the same wealth distribution and colours' legend of the previous section 3.7.2 is reported in figure 3.5.

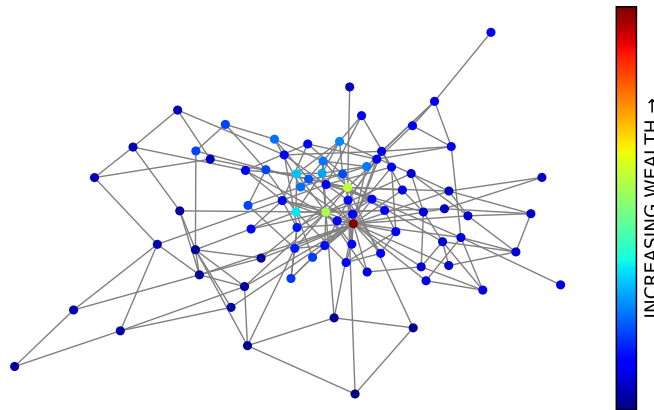


Figure 3.5: Complete Network of 81 agents for Fisk wealth distribution with $\alpha = 1$, $\beta = 2.2$, $q = 0.6$ and $MC = 0.5$.

3.8 Media effect

The robust social network permeating modern world collectivities is psychologically shaping our beliefs, persuading mass opinion and orientating everyday life decision making, the portrait of a powerful but delicate self-propelling hype machine described by Aral [37]. Preceding this dense interconnected tissue of opinions dissemination, the Mass Media fulfils the director's role by selecting the nature and conveyance modality of information. Media policy has concrete rebounds in social behaviour as illustrated by Vasterman et al. [38] in terms of impact in the Aftermath of Disasters. The news magnification of terrorist actions after the Oklahoma City bombing in 1995, for example, directly impacted the spread of post-traumatic

stress symptomatologies in children exposed to television viewing [39] even if geographically distant from the explosion [40]. Although the technological development of the modern world allows media to access a wide range of information directly, the profit model underlying their practices determines management by extremes attitudes such that media, merchants of attention [41], tend to select the worst frightening news, enormously overestimating the probability of rare events. In the XY model we propose for opinions' dynamics, the media act as a time-dependent random field pointing toward the y axis communicating bad news that naturally reduce the individual propensity to invest in a risky opportunity. The same harmonic operation we illustrated for social couplings gives the intensity of the media field perceived by each agent, representing how wealthy people have stronger opinions and are less likely to be influenced by public information, differently from the poor. If we consider an agent i at time t with wealth $W_i(t)$ she will feel a media field:

$$\vec{h}_{\text{media},i}(t) = (W_i(t)/W_M(t)) \hat{u}_y \quad (3.18)$$

where \hat{u}_y is the y -axis unitary vector while $W_M(t)$ represent the content of media news. As discussed in the introduction, the individual risk propensities update at the end of any investment realisation through the Montecarlo evolution of the system with previously discussed Hamiltonian (Eq. 3.4). In particular, after disclosing the investments' returns, the wealth of each agent changes (gain or loss), implying an adjustment in both idiosyncratic and media fields. According to their utilitarian nature, media are supposed to collect wealth losses and report them in a weighted way such that the *gamma media* (Γ_{media}) parameter describes the extent of management by extremes. The information content conveyed by media is thus:

$$v(t) = \sum_{i=1}^{\Gamma_{\text{media}}} \frac{|\Delta W_{i,\text{loss}}(t)|}{\Gamma_{\text{media}}}, \quad |\Delta W_{i,\text{loss}}(t)| > |\Delta W_{i+1,\text{loss}}(t)| \quad (3.19)$$

$$\Delta W_{i,\text{loss}}(t) = \begin{cases} 0 & \text{if } W_i(t) > W_i(t-1) \\ W_i(t) - W_i(t-1) & \text{otherwise} \end{cases} \quad (3.20)$$

It is trivial to check that if Γ_{media} equal to 1 the media reports just the worst loss (extreme management by extremes), instead if Γ_{media} is large media honestly reports an average of all the losses. Finally media convey news on the basis of what happened in the previous T days. The way we can account for this is a weighted sum of the previous news with a memory discount factor β that explains the complete expression of term $W_M(t)$ in equation 3.18:

$$W_M(t) = \sum_{k=0}^T \beta^k v(t-k), \quad \beta \in [0, 1] \quad (3.21)$$

3.9 Control parameters

To sum up, considering a society with power-law wealth distribution and an appropriate degree of wealth inequality, we combined idiosyncratic and media fields with a scale-free interacting system designing a realistic picture of a human network for risk-aversion spreading. Indeed we introduced appropriate physical parameters embodying the fundamental reasons underlying the birth of the zero-risk society, as described in table 3.1. The proposed measures act as suitable tuning knobs tracing the evolution of human communities while in a more physical framework have the role of control parameters for the random field XY model.

INGREDIENTS OF THE ZERO RISK SOCIETY	CONTROL PARAMETERS OF THE XY MODEL
WELFARE STATE	α AND β IN FISK WEALTH DISTRIBUTION
NO ACCESS TO OPPORTUNITIES	POVERTY THRESHOLD
HERDING AND IMITATION	MEDIA CONNECTIVITY
MANAGEMENT SHAPED BY EXTREMES AND OVERREACTION	GAMMA MEDIA (Γ_{media})

Table 3.1: Mapping between zero-risk society ingredients and XY model control parameters.

Chapter 4

Simulations

4.1 Model dynamics

The designed model evolves dynamically with a cyclic alternation of wealth updates (with the exponential Ornstein Ulhenbeck process at stationarity) controlled by the individual risk propensity a (Eq. 2.14-2.16) and opinions' revising through the XY model that has been simulated in a Montecarlo algorithm at temperature $T=0$. On each day, the outcomes of the risky assets are disclosed; namely, new wealths are picked from the log-normal distribution and opinions update for the subsequent investments. The first steps of the simulation are:

- Initial condition (Day 0): Wealth capitals are sampled from the Fisk distribution and assigned to each agent. According to her idiosyncratic field, any individual allocates a fraction a of wealth to the risky asset before interacting with other investors. Therefore, as expressed in equation 3.10, wealthy people (rarely sampled from the power-law tail of the Fisk distribution) have their spins more oriented along the vertical axis rather than poor as observable in figure 4.1 reporting the initial spins' alignment in a fictitious 2D grid. A fraction of people struggling to survive can not access the market opportunities; they do not invest in the risky option and are represented by magenta spins fixed on the y-axis.
- Day 1: At the beginning of day 1, each agent receives a new wealth extracted from her proper Log-normal distribution with volatility (standard deviation) proportional to her risk propensity on the previous day. According to the new capital, all the investors change their idiosyncratic fields, the media fields turn on reporting the worst losses of the day and people interact, determining a new set of $\{a_i\}_{i=1}^N$ values for the population.
- Day 2: At the beginning of day 2, given yesterday's investments, agents mod-

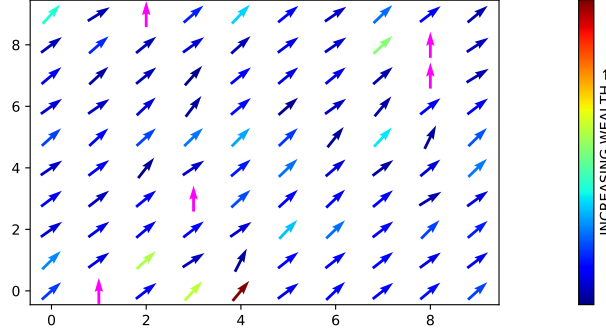


Figure 4.1: Initial spin configuration for 100 agents. Magenta spins do not invest.

ify again their wealths which induces a new opinion processing. The same mechanisms characterize the following days of the simulation.

4.2 Results

After an intensive theoretical investigation, we devised an optimized and parallelized Python3 code to simulate the model. We numerically reproduced the system dynamics for a large spectrum of parameters averaging over many seeds of the random number generation to test the robustness of its conclusions. In the following, we will report and comment on the simulation results for a system with 400 interacting agents in a scale-free social media network (with $m = 2$ in the Bianconi Barabasi algorithm) and Fisk wealth distribution, with $\alpha = 1$ (3.6). The utility parameter $\sigma = 0.5$ (3.10), $slope = 0.1$ (3.8) for the access to opportunities probability, $q = 0.8$ in the local network structure and $\beta = 0.9$ (3.21) for the social media memory effect. The simulation has been carried for 500 days.

Setting $poverty\ threshold = 0.05$, we plotted the average value of the equilibrium risk propensities (3.5) as a function of the remaining control parameters, time averaging over the last 20% of the simulation steps to guarantee the achievement of a stable behaviour. For $\beta = 2.2$ in the log-logistic law, as displaced in figure 4.2a the order parameter strongly decreases with the reduction of $gamma\ media$, namely with the amplification of the management by extremes tendency of mass media. Furthermore, social imitation and herding actively contributes to reducing risk propensity in the population. In 4.2b, instead, by fixing the $media\ connectivity = 1$, we observed how the increase in wealth inequality, reduction of β in the Fisk distribution, strongly impact the diffusion of a risk-averse mindset.

Successively we fixed the parameter of wealth distribution to $\alpha = 1$ and $\beta = 2.2$ and

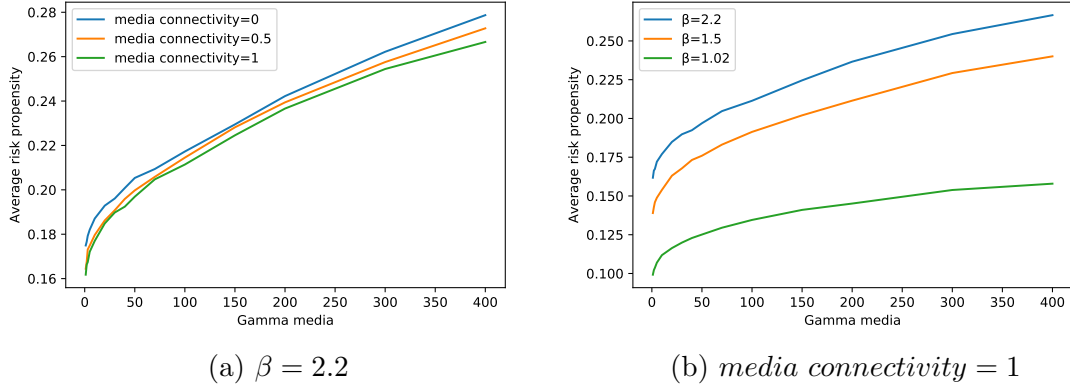


Figure 4.2: Average risk propensity vs *gamma media*, for different values of *media connectivity* and β in Fisk distribution. *Poverty threshold* = 0.05.

analysed the risk propensity behaviour with respect to the *poverty threshold*, precisely the percentage of the population that, due to wealth inequality, can not access risk investment opportunities. At fixed *gamma media* = 50 the average (over the agents and in time) risk attitude significantly diminishes if the *poverty threshold* grows with a clear reducing impact of social media interactions, as illustrated in figure 4.3a. Moreover, for a strongly interconnected society (figure 4.3b), management by extremes, expressed by small values of *gamma media*, affects the collective opinion conveying a risk-averse perspective for any value of *poverty threshold*.

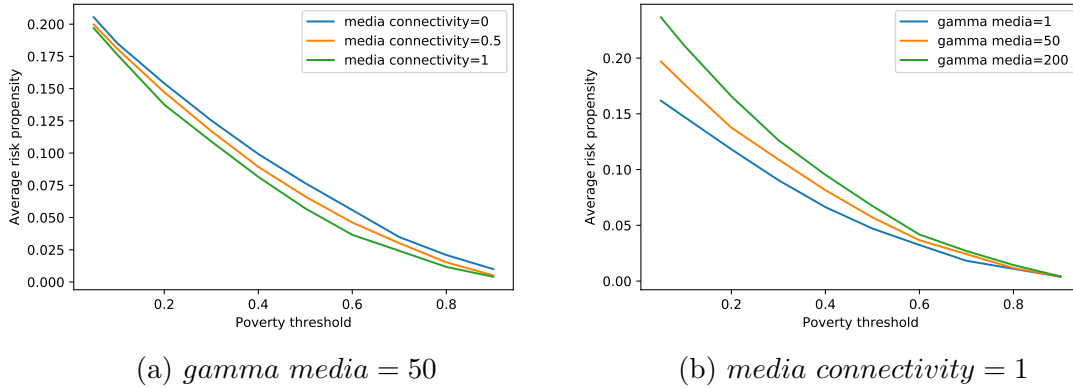
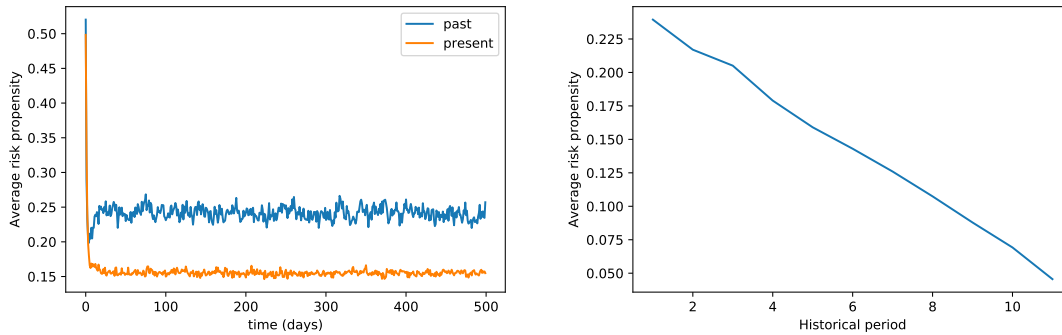


Figure 4.3: Average risk propensity vs *Poverty threshold*, for different values of *media connectivity* and *gamma media*. $\alpha = 1$ and $\beta = 2.2$ in the Fisk wealth distribution.

Finally, in the last panel we report the evolution of the average risk propensity in

several historical periods. Figure 4.4a illustrates the time evolution of \bar{a} comparing past and present days. In details, we modified together the four control parameters of the model to mimic the transition from a risk-taking scenario with $\bar{a} \approx 0.24$ to a zero-risk society with $\bar{a} \approx 0.16$. We used $\beta = 4.2$, *poverty threshold* = 0.05, *gamma media* = 400 and *media connectivity* = 0 for the past (indicatively modelling the beginning of the past century) while $\beta = 2.2$, *poverty threshold* = 0.10, *gamma media* = 5 and *media connectivity* = 1 to describe the modern society. In figure 4.4b, instead, we present the continuous dynamical evolution of the average risk propensity (averaged in last 20% time steps of the simulation) across history, ideally describing the transition from early 1900 to nowadays and future societies. The x-axis is a fictitious scale indicating the transition from past, leftmost side of the axis to future, rightmost side. We adopted a continuous shift of the control parameters that simulate an increase in wealth inequality, a reduced access to opportunities, a more prominent social media connectivity and a massive mind-controlling public information influence through management by extremes and overreaction. The combination of the four factors, as hypothesised, definitely pushed the contemporary world to a reduction of the risk-taking nature essential for innovation: we live in a zero-risk society.



(a) Time evolution of the average risk propensity in past and present days (b) Scan of human history, leftmost (rightmost) x-axis represents past (future)

Figure 4.4: Average risk propensity in several historical periods.

The intensive numerical simulations revealed remarkable robustness of the model results concerning some changes in the number of involved agents. Although the Zero-risk factors reduce average risk propensity in any population, this effect is stronger in a wide community than in a small social group due to the higher wealth inequality and the consequent higher media probability of detecting and spreading terrible losses.

Chapter 5

Covid model

The model we designed to describe the transition of modern societies into a zero-risk environment can be easily adapted and detailed to explain the social response to Covid19 and its difference from the human reaction to past worldwide diseases. In details, we have substituted the investment layer of our network based on the allocation of capital resources in a risky asset and the stochastic evolution of its return with a SIRD model for epidemic spreading. Our analysis extends the bilayered network proposed by Fast et al. [42] to illustrate the development of social responses during a pandemic by introducing the reverse rebound of ideas diffusion on the pandemic state itself. As far as the dynamical model for disease diffusion is concerned, we added a death state (D) to the Susceptible-Infected-Recovered (SIR) model for epidemic spreading [43] in a scale-free Network [44]. Especially we designed a scale-free network of subpopulations or cities [45], [46] with random graph modelling social connectivity inside single clusters. Agents can spread the virus by moving inside their metapopulation and travelling abroad, with a probability of getting in touch with other individuals that depend on their risk propensity; the latter evolves with the zero temperature MonteCarlo dynamics of the XY opinion model, as in the original Zero-risk picture. Figure 5.1, from Francesco Maria Russo Master Thesis, illustrates the model states and possible transitions. Infected agents after a deterministic time T_I die or become recovered with probabilities P_{ID} and P_{IR} that depend on the age through a nonlinear sigmoid function. At each time step, every recovered agent has a certain probability P_{RS} to become susceptible again. We adopted the previously detailed XY model to describe opinion dynamics. Indeed we associated the spin angle of any agent to the probability of exiting home undergoing external social interactions during the pandemic, a measure of the individual risk propensity:

$$\vec{s}_i = (\cos(\theta_i), \sin(\theta_i)); \quad \theta_i = \frac{\pi}{2} [1 - P_i(exit)] \quad (5.1)$$

The resulting order parameter will be the average exit probability in the whole

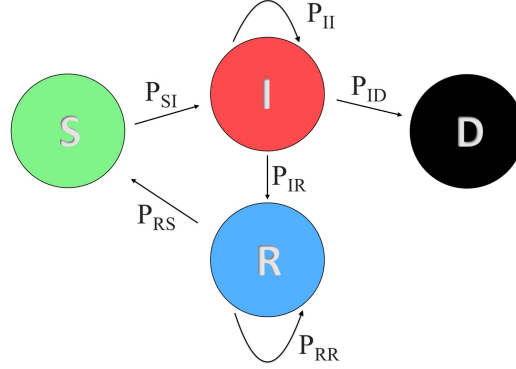


Figure 5.1: SIRD model states and possible transitions.

population. After normalizing the age distribution, we introduced the health capital parameter Θ equal to one minus the age such that young agents have high health capital (Θ close to 1) while older people show small Θ values. In this framework, idiosyncratic fields \vec{h} continue to model individual risk propensities and result in a decreasing function of the individual health capital Θ weighted by a step function of the health status $f(X)$:

$$\vec{h}_i(t) = |\vec{h}_i(t)| (\cos(\theta_i^*), \sin(\theta_i^*)) \quad (5.2)$$

$$\theta_i^* = \frac{\pi}{2} (1 - P_i(\text{Exit}^* | \Theta_i, X_i)) \quad (5.3)$$

$$P_i(\text{Exit}^* | \Theta_i, X_i) = \Theta_i f(X_i), \quad X_i \in \{S, I, R, D\} \quad (5.4)$$

$$f(X_i) = \begin{cases} 1 & X_i = S, R \\ \frac{1}{2} & X_i = I \\ 0 & X_i = D \end{cases} \quad (5.5)$$

The field modulus is described by the product of health capital and social connectivity, accounting for the fact that younger and more influential individuals have stronger personal opinions. The coupling terms of the model represent social communications and the impacts of social interaction and mass media pressure on each agent are weighted by the parallel operation of equation 3.18 where wealth is replaced by a combination of health capital Θ and degree of social media interconnection k :

$$J_{ij} = (\Theta_i // \Theta_j)(k_i // k_j) \quad (5.6)$$

Therefore more influential individuals, together with very young guys, are less likely to be influenced rather than older and less connected adults. At the same time, mass media would achieve its opportunistic purposes by focusing on the very sporadic

deaths of young citizens (management by extremes), conveying a state of fear and risk aversion. We traced the dynamics of human society by substituting the wealth evolution of the zero-risk society model with the progression of age distribution that showed a considerable increase of the median age from 1950 data to 2050 projections [47]. Therefore for fixed-parameters specifying the pandemic spreading, we analysed how new age distribution, robust media connectivity and media management by extremes deeply affected the average risk propensity, which heavily reduced over the last decades. This study explains why the social reaction to Covid19 has been very different from the human response to similar past pandemics like the 1957-1958 Asian flu. The complete theoretical details and simulation results of the Covid model are discussed in the Master Thesis of my friend and colleague Francesco Maria Russo while the parallelisms between the Zero-risk society model and the Covid model are reported in table 5.1.

ZERO RISK SOCIETY MODEL	COVID MODEL
WEALTH DISTRIBUTION	AGE DISTRIBUTION
OU PROCESS FOR WEALTH EVOLUTION	SIRD MODEL FOR HEALTH EVOLUTION
NO ACCESS TO OPPORTUNITY	DECEASED AGENTS
$(\vec{s}_i)_x$ ENCODING RISK PROPENSITY IN INVESTING IN THE RISKY ASSET	$(\vec{s}_i)_x$ ENCODING RISK PROPENSITY AS EXIT PROBABILITY
IDIOSYNCRATIC FIELDS ARE INDIVIDUAL RISK PROPENSITIES BASED ON WEALTH	IDIOSYNCRATIC FIELDS ARE INDIVIDUAL RISK PROPENSITIES BASED ON AGE AND HEALTH
HERDING AND IMITATION, WEALTHY AGENTS ARE LESS INFLUENCED	HERDING AND IMITATION, YOUNG AGENTS ARE LESS INFLUENCED
MEDIA FOCUS ON THE WORST LOSSES (MANAGEMENT BY EXTREMES)	MEDIA FOCUS ON YOUNG DEATHS (MANAGEMENT BY EXTREMES)
MONTE CARLO SIMULATION FOR INFORMATION SPREADING	MONTE CARLO SIMULATION FOR INFORMATION SPREADING

Table 5.1: Parallelisms between Zero-risk society model and Covid model

Chapter 6

Conclusion and perspectives

We designed a model that describes how the increased social welfare, wealth inequality and no access to opportunities, social media interactions, and media management by extremes across human history let the society evolve to a risk-averse panorama, with scarce desire to explore new unknown, risky landscapes. This decadent attitude, exhaustively displaced by the social reaction to the Covid19 pandemic, profoundly threatens modern civilisation's robustness that increasingly resembles a static apparatus completely unprepared to handle the unstable volatility of its environment. Although the numerical results validate the model capability to reproduce the hypothesised mechanism, we need further simulations to explore the completeness of control parameter space. This exploration will be essential to find potential regions with a non-trivial behaviour of the order parameter whose functional shape we hope will match the typical phase transitions observed in the Ising-like models. Moreover, by introducing a suitable symmetrisation, we could remove the first quadrant constraint of the designed XY model, looking for the presence of a Berezinskii–Kosterlitz–Thouless transition [21] and the consequent typical vortex structure, to be appropriately interpreted.

Bibliography

- [1] Didier Sornette and Peter Cauwels. Trapped in the “zero-risk” society and how to break free(1st Sept. 2020) Swiss Finance Institute Research Paper No. 20-78, Available at SSRN: <https://ssrn.com/abstract=3684550> published in german as “Gefandan in der Null risiko-gesellschaft” (Caught in the zero-risk society), Twice, Herbst 2020, pp. 4-7.
- [2] Didier Sornette and Guy Ouillon. Dragon-kings: mechanisms, statistical methods and empirical evidence. *The European Physical Journal Special Topics*, 205(1):1–26, 2012.
- [3] Daniel Bernoulli. Exposition of a new theory on the measurement of risk. *Econometrica*, 22(1):23–36, 1954.
- [4] Kenneth J Arrow. The theory of risk aversion. *Essays in the theory of risk-bearing*, pages 90–120, 1971.
- [5] Danyang Xie. Power Risk Aversion Utility Functions. Technical report, University Library of Munich, Germany, 2002.
- [6] Jan Von Plato. Boltzmann’s ergodic hypothesis. *Archive for History of Exact Sciences*, 42(1):71–89, 1991.
- [7] Ole Peters. Optimal leverage from non-ergodicity. *Quantitative Finance*, 11(11):1593–1602, Nov 2011.
- [8] William Feller. *An Introduction to Probability Theory and Its Applications*, volume 1. Wiley, January 1968.
- [9] Ömer Önalán. Financial modelling with ornstein - uhlenbeck processes driven by levy process. *Lecture Notes in Engineering and Computer Science*, 2177, 07 2009.
- [10] Eduardo S Schwartz. The stochastic behavior of commodity prices: Implications for valuation and hedging. *The Journal of finance*, 52(3):923–973, 1997.
- [11] Alan P. Kirman. Whom or what does the representative individual represent? *Journal of Economic Perspectives*, 6(2):117–136, June 1992.

- [12] Serge Galam. Rational group decision making: A random field ising model at $t = 0$. *Physica A: Statistical Mechanics and its Applications*, 238(1-4):66–80, Apr 1997.
- [13] D.P. Belanger and A.P. Young. The random field ising model. *Journal of Magnetism and Magnetic Materials*, 100(1):272–291, 1991.
- [14] Yusuf Yüksel, Erol Vatansever, Ümit Akinci, and Hamza Polat. Nonequilibrium phase transitions and stationary-state solutions of a three-dimensional random-field ising model under a time-dependent periodic external field. *Phys. Rev. E*, 85:051123, May 2012.
- [15] Muktish Acharyya. Nonequilibrium phase transition in the kinetic ising model: Dynamical symmetry breaking by randomly varying magnetic field. *Phys. Rev. E*, 58:174–178, Jul 1998.
- [16] Q. Michard and J.-P. Bouchaud. Theory of collective opinion shifts: from smooth trends to abrupt swings. *The European Physical Journal B*, 47(1):151–159, Sep 2005.
- [17] DA Garanin, EM Chudnovsky, and T Proctor. Random field x y model in three dimensions. *Physical Review B*, 88(22):224418, 2013.
- [18] Mario J de Oliveira. Isotropic majority-vote model on a square lattice. *Journal of Statistical Physics*, 66(1):273–281, 1992.
- [19] André Vilela and H. Stanley. Effect of strong opinions on the dynamics of the majority-vote model. *Scientific Reports*, 8, 06 2018.
- [20] L Costa and Adauto Souza. Continuous majority-vote model. *Physical review. E, Statistical, nonlinear, and soft matter physics*, 71:056124, 06 2005.
- [21] John Michael Kosterlitz and David James Thouless. Ordering, metastability and phase transitions in two-dimensional systems. *Journal of Physics C: Solid State Physics*, 6(7):1181, 1973.
- [22] Juan Carlos González-Avella, Mario G. Cosenza, Konstantin Klemm, Víctor M. Eguíluz, and Maxi San Miguel. Information feedback and mass media effects in cultural dynamics. *Journal of Artificial Societies and Social Simulation*, 10(3):9, 2007.
- [23] Joachim Hubmer, Per Krusell, Anthony A Smith, et al. The historical evolution of the wealth distribution: A quantitative-theoretic investigation. Technical report, National Bureau of Economic Research, 2017.
- [24] Christoph Lakner and Branko Milanovic. Global Income Distribution: From the Fall of the Berlin Wall to the Great Recession. *The World Bank Economic Review*, 30(2):203–232, 08 2015.

- [25] Emmanuel Saez and Gabriel Zucman. Wealth inequality in the united states since 1913: Evidence from capitalized income tax data. Working Paper 20625, National Bureau of Economic Research, October 2014.
- [26] Peter R. Fisk. The graduation of income distributions. *Econometrica*, 29(2):171–185, 1961.
- [27] Corrado Gini. On the measure of concentration with special reference to income and statistics. *Colorado College Publication, General Series*, 208(1):73–79, 1936.
- [28] Peter J. Cameron. *The Random Graph*, pages 333–351. Springer Berlin Heidelberg, Berlin, Heidelberg, 1997.
- [29] Albert-László Barabási and Eric Bonabeau. Scale-free networks. *Scientific American*, 288(5):60–69, 2003.
- [30] Mark Steyvers and Joshua Tenenbaum. The large-scale structure of semantic networks: Statistical analyses and a model of semantic growth. *Cognitive science*, 29:41–78, 01 2005.
- [31] Réka Albert and Albert-László Barabási. Statistical mechanics of complex networks. *Rev. Mod. Phys.*, 74:47–97, Jan 2002.
- [32] G Bianconi and A.-L Barabási. Competition and multiscaling in evolving networks. *Europhysics Letters (EPL)*, 54(4):436–442, may 2001.
- [33] Ginestra Bianconi and Albert-László Barabási. Bose-einstein condensation in complex networks. *Phys. Rev. Lett.*, 86:5632–5635, Jun 2001.
- [34] Miller McPherson, Lynn Smith-Lovin, and James M Cook. Birds of a feather: Homophily in social networks. *Annual Review of Sociology*, 27(1):415–444, 2001.
- [35] Lois Verbrugge. The structure of adult friendship choices. *Social Forces*, 56:576, 12 1977.
- [36] Augustine Pang. Social media hype in times of crises: Nature, characteristics and impact on organizations. *Asia Pacific Media Educator*, 23(2):309–336, 2013.
- [37] Sinan Aral. *The Hype Machine*. Random House US, 2021.
- [38] Peter Vasterman, C Joris Yzermans, and Anja JE Dirkzwager. The role of the media and media hypes in the aftermath of disasters. *Epidemiologic reviews*, 27(1):107–114, 2005.
- [39] Betty Pfefferbaum, Sara Jo Nixon, Rick D Tivis, Debby E Doughty, Robert S Pynoos, Robin H Gurwitch, and David W Foy. Television exposure in children after a terrorist incident. *Psychiatry: Interpersonal and Biological Processes*, 64(3):202–211, 2001.

- [40] Betty Pfefferbaum, Thomas W Seale, Nicholas B McDonald, Edward N Brandt Jr, Scott M Rainwater, Brian T Maynard, Barbara Meierhoefer, and Peteryne D Miller. Posttraumatic stress two years after the oklahoma city bombing in youths geographically distant from the explosion. *Psychiatry*, 63(4):358–370, 2000.
- [41] Tim Wu. *The Attention Merchants: The Epic Scramble to Get Inside Our Heads*. Deckle Edge, 2016.
- [42] Shannon Fast, Marta C. Gonzalez, James Wilson, and Natasha Markuzon. Modelling the propagation of social response during a disease outbreak. *Journal of the Royal Society, Interface / the Royal Society*, 12, 03 2015.
- [43] Tiberiu Harko, Francisco S.N. Lobo, and M.K. Mak. Exact analytical solutions of the susceptible-infected-recovered (sir) epidemic model and of the sir model with equal death and birth rates. *Applied Mathematics and Computation*, 236:184–194, Jun 2014.
- [44] Romualdo Pastor-Satorras and Alessandro Vespignani. Epidemic spreading in scale-free networks. *Physical Review Letters*, 86(14):3200–3203, Apr 2001.
- [45] Jessica T Davis, Nicola Perra, Qian Zhang, Yamir Moreno, and Alessandro Vespignani. Phase transitions in information spreading on structured populations. *Nature physics*, 16(5):590–596, 2020.
- [46] Vittoria Colizza and Alessandro Vespignani. Epidemic modeling in metapopulation systems with heterogeneous coupling pattern: Theory and simulations. *Journal of Theoretical Biology*, 251(3):450–467, 2008.
- [47] Population pyramids of the world from 1950 to 2100. <http://populationpyramid.net>.